Asian Journal of Chemistry; Vol. 33, No. 2 (2021), 465-470

ASIAN JOURNAL OF CHEMISTRY

https://doi.org/10.14233/ajchem.2021.22932

Synthesis of Visible Light Active Delafossite Structured $CuCrO_2$: Optical and Photocatalytic Studies

NAGARAJAN ARUNKUMAR

P.G. & Research Department of Chemistry, Saraswathi Narayanan College, Madurai-625022, India

Corresponding author: E-mail: arun.snc.mdu@gmail.com

Received: 6 August 2020; *Accepted*: 2 January 2021; *Published online*: 15 January 2021; AJC-20236

Synthesis of delafossite structured $CuCrO_2$ by sol-gel method using tartaric acid as a complexing agent is reported in present study. The product has been characterized by powder X-ray diffraction, thermal analysis (TGA/DTA), SEM, Raman spectra, BET (surface area analysis) and UV-Vis-diffused reflectance spectroscopy. Powder X-ray diffraction revealed the formation of delafossite structured $CuCrO_2$ phase at 800 ºC for 3 h, which was further confirmed by thermal analysis that showed one weight loss and endothermic peak at above 800 ºC corresponded to the phase transition. Hexagonal plate like morphology of the synthesized powder was confirmed by SEM analysis. The Raman spectra showed three Raman scattering peaks of the delafossite structure of $CuCrO_2$. Diffused reflectance spectroscopy (DRS) revealed that the band gap of the prepared $CuCrO_2$ microcrystals was about 2.90 eV. In addition, the synthesized $CuCrO_2$ was used for the degradation of *p*-nitrophenol and H_2 generation under visible-light which showed 32.4 µmol (10.8 µmol/h) of H_2 and 92 % degradation of *p*-nitrophenol (20 mg/L) after 4 h of visible light irradiation. Further analysis revealed that $^{\bullet}OH$ and $^{\bullet}O_2^-$ were the main ROS responsible for *p*-nitrophenol degradation.

Keywords: Delafossite structure, $CuCrO_2$, Optical properties, Degradation, *p*-Nitrophenol.

INTRODUCTION

Transparent conducting oxides (TCOs) are exclusive materials that organize electrical conductivity and optical transparency in a single material [1]. Among TCOs semiconductos, n-type semiconductors have defects such as impurity substitutions, making oxygen vacancies and interstitials donate electrons to the conduction band provided that charge carriers for the stream of electric current (*e.g.* ZnO, In_2O_3, SnO_2, *etc.*) [2]. In p-type TCO semiconductor materials, hole doping by impurity acceptor ion substitutions, ionized cation vacancies and oxygen inter-stitials act as electron acceptors (*e.g.* $CuAlO_2$, $CuGaO_2$, $CuCrO_2$, *etc.*). Studies on delafossite oxides are interesting not only for the transparent conducting oxides but also having wide range of applications such as in sensor materials, dilute magnetic semiconductor, catalytic and thermoelectric material [3-7]. Delafossite compounds belong to a family of general formula ABO_2 structured ternary oxides. Delafossite semi-conducting metal oxide in the chemical form of $M^I M^{III} O_2$, where M^I is a monovalent cation (*e.g.* Cu^+, Ag^+) and M^{III} is a trivalent cation (*e.g.* Al^{3+}, In^{3+}, Cr^{3+}, Co^{3+}, Fe^{3+}, Ga^{3+}, *etc.*) [8]. The ABO_2 delafossite structure can be labelled as a stacking of BO_2 layers made of edge-sharing BO_6 octahedra that are connected by planes of A^+ cations ordered as a triangular network. All the cation A^+ is linearly coordinated by two anions O^- going to the upper and lower BO_2 layers. The oxygen layers can be stacked in dissimilar ways along the *c*-xis in order to form two types of delafossite structure (a) rhombohedral 3R (space group R3m) polytypes, and (b) hexagonal 2H (space group$P6_3/mmc$) [9]. $CuCrO_2$ is a more capable transport conducting oxide (TCO) than $CuFeO_2$ because of its significant optical transparency in the visible range with a band gap of about 3.1 eV and electrical conductivity that can be extremely enhanced up to σRT = 220 S/cm with suitable doping like $CuCr_{0.95}Mg_{0.05}O_2$ thin film [10].

In few last years, Deng *et al.* [11] synthesized bulk and thin $CuCrO_2$ films by sol-gel method and pulse laser deposition in which the structural, optical, electrical properties and ozone sensing properties were studied. Dupont *et al.* [12] reported the synthesis of $CuCrO_2$ by sol-gel method using

propionic acid as gelling agent and also investigated its catalytic properties. Li *et al*. [13] synthesized Mn doped $CuCrO_2$ by sol-gel method and investigated the electrical, magnetic and paramagnetic properties in the temperature range of 120-300 K. Zhou *et al*. [14] reported the existence of delafossite $CuCrO_2$ in nanocrystalline and microcrystalline state, which was prepared by hydrothermal and sol-gel methods. The synthesis of nano-sized $CuCrO_2$ porous powders by combustion process using glycine nitrate as a fuel is reported by Chiu *et al*. [15]. Jlaie *et al*. [16] reported the polycrystalline $CuCr_{0.95}M_{0.05}O_2$ (M = Al, Co, Rh and Sc) samples, which was prepared by solid-state synthesis and the magnetic susceptibility of complete samples exhibited paramagnetic nature at high temperature. Herein, delafossite $CuCrO_2$ was synthesized by sol-gel process using tartaric acid as a complexing agent and its photocatalytic degradation was also investigated.

EXPERIMENTAL

The starting precursor materials used for the synthesis of $CuCrO_2$ were copper nitrate ($Cu(NO_3)_2{\cdot}3H_2O$; 99.5%) (Himedia, India), chromium nitrate ($Cr(NO_3)_3{\cdot}9H_2O$; 98%) (Thomas beaker, India), methanol (Mecrk) and tartaric acid (Aldrich 99.9%) were obtained.

Preparation of $CuCrO_2$: Copper nitrate and chromium nitrate were mixed in a 1:1 M ratio followed by the addition of 30 mL of methanol at room temperature. Then 4 M of tartaric acid dissolved in 30 mL of deionized water was added to the above homogeneous metal nitrate mixture slowly and the mixture was stirred for 2 h to obtain well-mixed precursor solution. The solution was again stirred at 80 ºC until jellification of solution was obtained followed by heating the gel until it becomes dried mass. Finally, the resulting solid was ground and heated at 500 ºC for 6 h to remove the organics. The obtained powder was then heated at 700 ° C/3, 6, 9 and12 h; and 800 ° C for 3h in air.

Characterization: The synthesized powders were characterized by Powder X-ray diffraction technique (XRD, BRUKER D8 ADVANCE, by CuKα radiation, λ = 1.5406 Å). The surface morphology and microstructure were examined by a scanning electron microscope (HRSEM-FEI Inspect F50). Thermal analysis (TA) of samples was recorded by TA SDTQ 600(USA) instrument. The samples were heated at 4 ºC/min up to 1000 ºC in nitrogen atmosphere. The standard BET (Micromeritics Gemini V) method was applied for measurement of the surface area. The Raman spectroscopy measurement was done by laser Raman spectrometer (HORIBA Scientific/Lab RAM HR). Diffused reflectance data were collected over the spectral range 200-2000 nm using (JASCO UV Vis NIR V-670, Japan).

Photocatalytic degradation of *p*-nitrophenol: The photocatalyst (20 mg) was dispersed in 100 mL of 20 mg/L *p*-nitrophenol. The suspension was then stirred in the dark condition for 30 min to achieve an adsorption/desorption equilibrium. Subsequently, the solution was then exposed with visible-light while stirring. The collected *p*-nitrophenol samples was finally analyzed by HPLC (Shimadzu, Japan) equipped with a Eclipse XDBC18 (4.6 × 150 mm, 5 µm) reverse phase column. The UV detector wavelength at 265 nm and the moveable phase consisted of methanol (50 %) and acetonitrile + acetic acid (50% + 1.6 mL/L) was fed at a flow rate of 1 mL min^{-1} for 20 min.

RESULTS AND DISCUSSION

Structural and morphological studies: The powder-XRD patterns of the sol-gel derived powders heated at 700 ºC for 12 h and 800 ºC for 3h in air are shown in Fig. 1. Secondary phase such as CuO and $CuCr_2O_4$ existing until powder was heated at 700ºC for 12h (Fig. 1a). The XRD spectra revealed the formation of delafossite structure $CuCrO_2$ phase at 800ºC after 3 h with rhombohedral symmetry (space group: $R\bar{3}m$) and lattice parameter value (a = 2.9921, c = 17.1616) and matched with standard (JCPDS card No. 039-0247) and no detectable impurity phase was observed (Fig. 1b). Product obtained by sol-gel method was less than the phase formation temperature by solid state reaction as reported earlier [4,14,18]. Using citric acid, in the sol-gel process, plays two different roles *i.e*. as a chelating agent and eludes the precipitation of hydroxylated compounds [19]. The metal nitrate-citrate process is a low temperature exothermic type oxidation-reduction reaction, where nitrates act as an oxidant and carbonyl groups of citric acid acted as a reducing agent [19]. In present case, tartaric

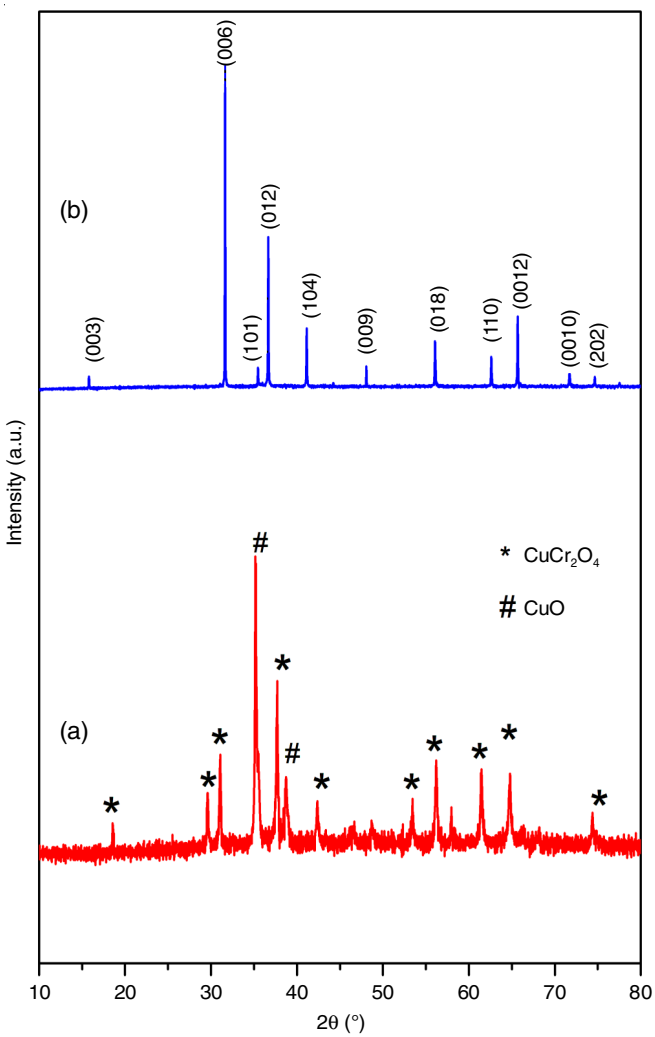

Fig. 1. XRD patterns of $CuCrO_2$ (a) 700 °C/12 h and (b) 800 °C/3h

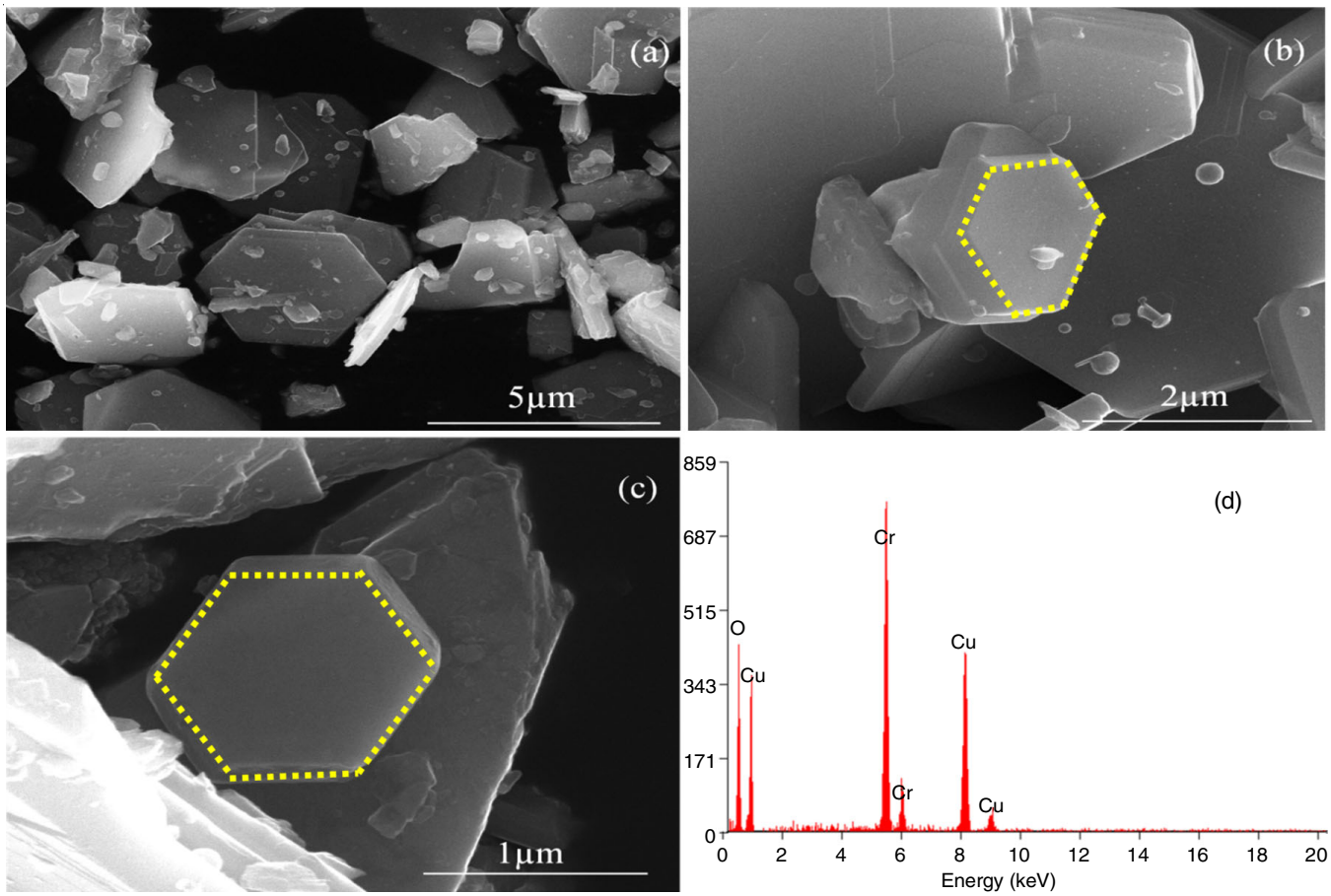

Fig. 2. SEM images (a-c) and EDX pattern (d) of $CuCrO_2$

acid was used, where nitrate ions act as an oxidant and carbonyl groups of tataric acid acted as a reducing agent in nitrate-tartrate route.

SEM studies: The surface morphology of synthesized $CuCrO_2$ powder exhibited a hexagonal shape plate like morphology (Fig. 2a-c). While, EDAX analysis showed all the elements present in the prepared powder (Fig. 2d). Furthermore, the BET surface area measurement revealed that the surface area of the prepared $CuCrO_2$ powder was about 1.05 m^2/g.

Thermal studies: The phase stability and thermal behaviour of $CuCrO_2$ powder were studied by (TGA/DTA) analysis under a nitrogen atmosphere at 4 ºC/min upto1000 ºC. The TGA thermogram (Fig. 3) shows one weight loss (5.16%) at 800 ºC and DTA gives one endothermic peak at 831 ºC, where the corresponding reaction occurred between copper monoxide (CuO) and cuprospinel ($CuCr_2O_4$) phases to form delafossite structure [20].

$$CuO + CuCr_2O_4 \longrightarrow 2CuCrO_2 + ½O_2$$

From the XRD pattern, a mixed phase of CuO and $CuCr_2O_4$ is present until powder is heated at 700 ºC for 12 h. The as-formed spinel and CuO phases reduced to delafossite $CuCrO_2$ at above 800 ºC. TGA curve show a percentage of weight loss of about 5% corresponding to the reduction of all Cu^{2+} ions to Cu^{+} ions. This reduction is systematically correlated to reaction pathway between spinel and monoxide to delafossite phase [21,22].

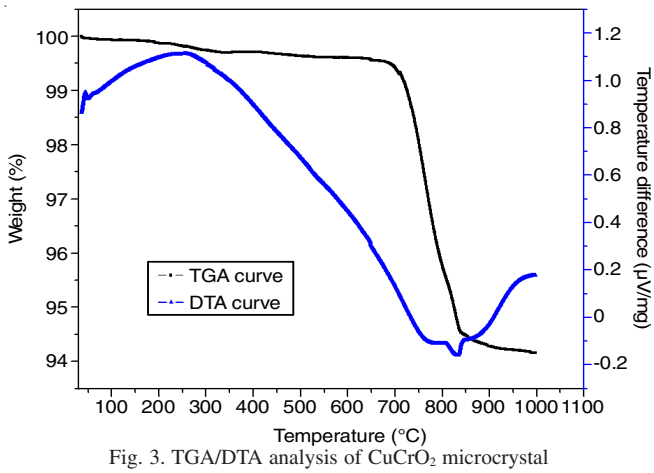

Fig. 3. TGA/DTA analysis of $CuCrO_2$ microcrystal

Raman studies: The delafossite structure belongs to point group C_{3v} and space group $R\bar{3}m$. The structure of $CuCrO_2$ powder was further investigated by Raman spectroscopy. The spectrum of $CuCrO_2$ shows three main vibration bands were observed corresponding to three scattering peaks 207, 441 and 689 cm^{-1}, respectively. The Raman spectroscopy results are consistent with the reported values [15]. They are identified as σ (A_{1g}), σ (E_g) and σ (A_g) at 689, 441 and 207 cm^{-1}, respectively (Fig. 4). It has been recommended that these vibrations may be related with the spectral features of edge-sharing $Cr^{III}O_6$ octahedra and possibly the O-Cu^{I}-O linear bond [23].

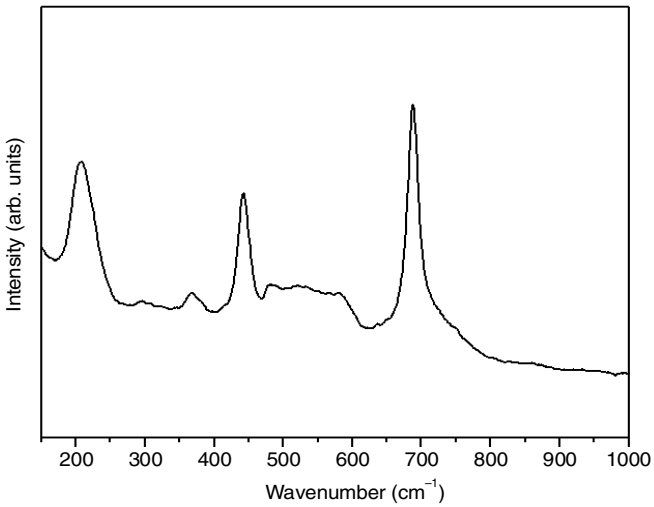

Fig. 4. Raman spectra of $CuCrO_2$ at room temperature

Optical properties: Optical properties of the sample were characterized by diffuse reflectance spectroscopy. The optical absorption spectrum of $CuCrO_2$ powder shows an absorption in the range of 400-500 nm (Fig. 5a). This value is near to the literature value [14]. The fundamental concept of absorption corresponds to excitation of electron from valance band to conduction band can be used to determine value of optical band gap of $CuCrO_2$ oxide.

In order to calculate the optical band gap of sample by using Tauc′s equation $(\alpha h\nu)^n = A(h\nu - E_g)$, where α denotes the absorption coefficient, $h\nu$ is the discrete photo energy, A is constant, E_g is band gap and exponent n depends on the type of the transition. For direct allowed transition, indirect allowed transition and direct forbidden transition, n is 1/2, 2 and 3/2, respectively [19,24]. Linear relationship between $(\alpha h\nu)^n$ and $h\nu$ indicates that optical band gap of $CuCrO_2$ (2.9 eV) (Fig. 5b). The optical band gap value is agreed with the literature value (2.95 eV) [14]. The reason is attributed to the different preparation methods [24,25].

Photocatalytic activity: The photocatalytic performance of the synthesized material was evaluated with visible light irradiation and *p*-nitrophenol as a demonstrative pollutant for the degradation. Fig. 6a depicts the UV-vis absorption spectra of *p*-nitrophenol at different time intervals. The absorption of

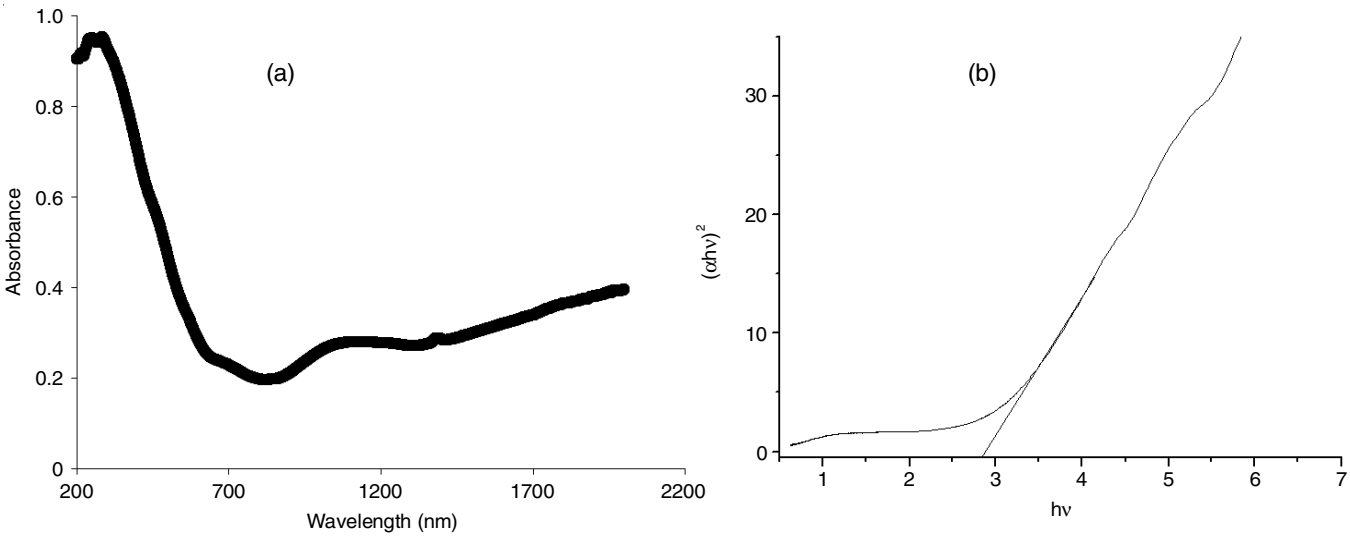

Fig. 5. (a) Optical absorption spectra (b) band gap curve of $CuCrO_2$ microcrystal

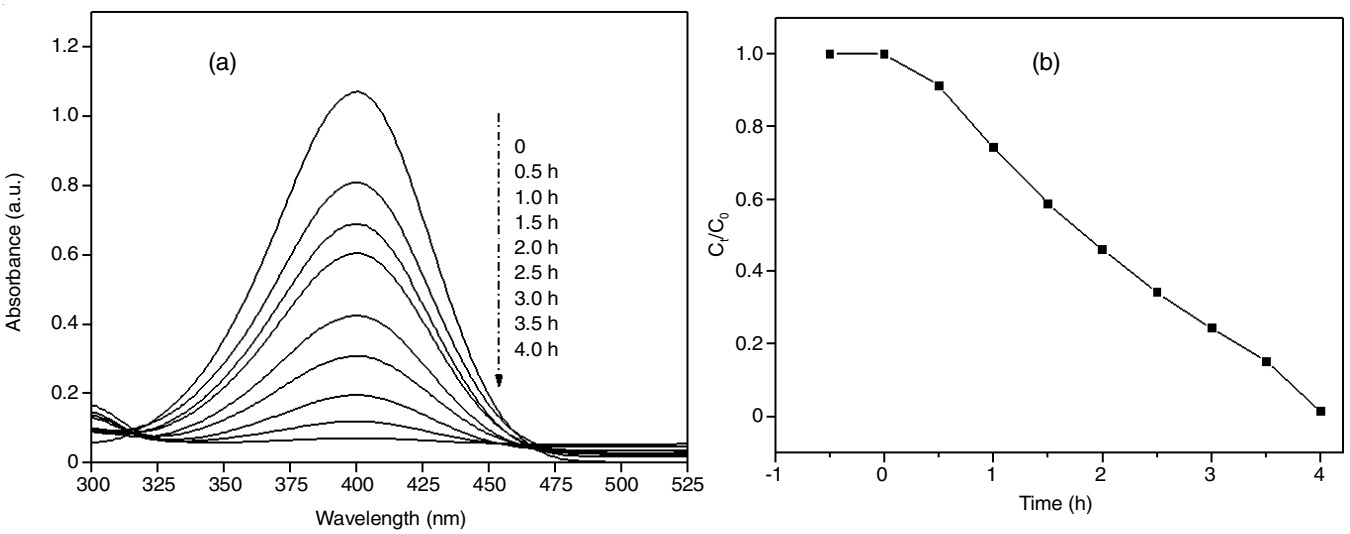

Fig. 6. (a) Temporal changes of *p*-nitrophenol (b) Percentage degradation of *p*-nitrophenol with respect to time

p-nitrophenol was decreased at 402 nm with increase in irradiation times and disappears completely after 4 h. Fig. 6b shows the relative concentrations of *p*-nitrophenol in the solution as a function of the irradiation time with different photocatalyst. The reaction kinetics of degradation of *p*-nitrophenol can be described by a Langmuir-Hinshelwood model (eqm.1), which showed that the reactions took place at a solid-liquid interface.

$$\ln\left(\frac{C_o}{C_t}\right) = k_r K_t = K_{apr} t \quad (1)$$

The degradation of *p*-nitrophenol under visible-light irradiation revealed a pseudo first-order kinetics with regression coefficients (R^2) ≥ 0.90 with rate constant k = 0.411 min^{-1}.

Photocatalytic degradation mechanism: A plausible photocatalytic degradation mechanism of $CuCrO_2$ was proposed and shown in Fig. 7. From the optical studies, the band gap value of $CuCrO_2$ was calculated to be around 2.9 eV. Thus, this compound could generate electron-hole pairs on activation by visible light which are responsible for photodegradation of pollutants. Upon irradiation, the photogenerated electron from valence band (VB) of $CuCrO_2$ excited to conduction band (CB) when reacted with the dissolved oxygen adsorbed on the surface of the photocatalyst to yield super oxide radicals $^{\bullet}O_2^-$, while h^+ reacted with the OH^- to generate hydroxide radicals $^{\bullet}OH$ [24,26], which further resulted for the degradation of *p*-nitrophenol into smaller molecules.

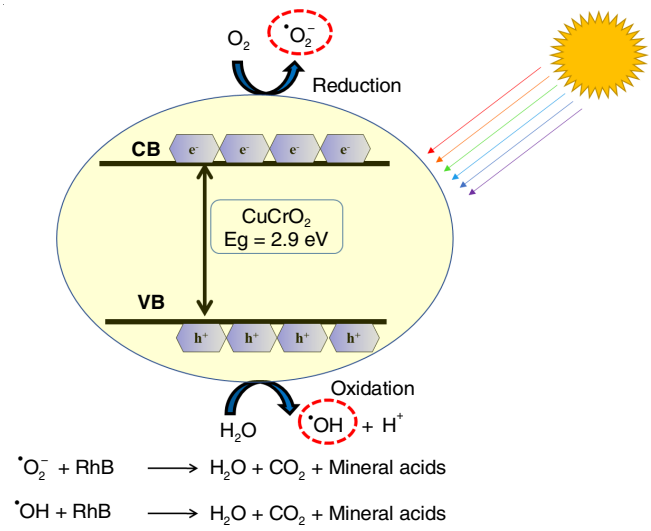

Fig. 7. Photocatalytic degradation mechanism of *p*-nitrophenol using $CuCrO_2$ microcrystal under visible light

Conclusion

In summary, a delafossite structured $CuCrO_2$ was successfully synthesized by sol-gel method using tartaric acid as a complexing agent at low temperature in the presence of air atmosphere. The XRD analysis confirmed the pure single phase $CuCrO_2$ with delafossite structure. The SEM-EDX analysis showed the morphology and composition of $CuCrO_2$ with hexagonal plate shape microcrystals. The thermal stability and reaction pathway between CuO and $CuCr_2O_4$ was investigated using thermal analysis. Raman spectra showed three Raman scattering peaks for delafossite structure of $CuCrO_2$. Furthermore, the prepared $CuCrO_2$ showed good photocatalytic activity towards degrading *p*-nitrophenol which could be utilized for other applications such as water splitting waste water treatment.

CONFLICT OF INTEREST

The authors declare that there is no conflict of interests regarding the publication of this article.

REFERENCES

1. A.N. Banerjee and K.K. Chattopadhyay, *Prog. Cryst. Growth Charact. Mater.*, **50**, 52 (2005); https://doi.org/10.1016/j.pcrysgrow.2005.10.001
2. J. Ding, Y. Sui, W. Fu, H. Yang, S. Liu, Y. Zeng, W. Zhao, P. Sun, J. Guo, H. Chen and M. Li, *Appl. Surf. Sci.*, **256**, 6441 (2010); https://doi.org/10.1016/j.apsusc.2010.04.032
3. S. Zhou, X. Fang, Z. Deng, D. Li, W. Dong, R. Tao, G. Meng and T. Wang, *Sens. Actuators B Chem.*, **143**, 119 (2009); https://doi.org/10.1016/j.snb.2009.09.026
4. M. Amami, F. Jlaiel, P. Strobel and A.B. Salah, *Mater. Res. Bull.*, **46**, 1729 (2011); https://doi.org/10.1016/j.materresbull.2011.05.033
5. T. Okuda, Y. Beppu, Y. Fujii, T. Kishimoto, K. Uto, N. Onoe, N. Jufuku, S. Hidaka, N. Teradal and S. Miyasaka, *J. Phys: Conf. Ser.*, **150**, 042157 (2009); https://doi.org/10.1088/1742-6596/150/4/042157
6. W. Ketir, A. Bouguelia and M. Trari, *Water Air Soil Pollut.*, **199**, 115 (2009); https://doi.org/10.1007/s11270-008-9864-z
7. T. Okuda, N. Jufuku, S. Hidaka and N. Terada, *Phys. Rev. B Condens. Matter Mater. Phys.*, **72**, 144403 (2005); https://doi.org/10.1103/PhysRevB.72.144403
8. N.A. Banerjee, K.C. Ghosh and K.K. Chattopadhyay, *Sol. Energy Mater. Sol. Cells*, **89**, 75 (2005); https://doi.org/10.1016/j.solmat.2005.01.003
9. A.M. Marquardt, N.A. Ashmore and D.P. Cann, *Thin Solid Films*, **496**, 146 (2006); https://doi.org/10.1016/j.tsf.2005.08.316
10. C.A. Rastogi, H.S. Lim and B. Desu, *J. Appl. Phys.*, **104**, 023712 (2008); https://doi.org/10.1063/1.2957056
11. Z. Deng, X. Fang, D. Li, S. Zhou, R. Tao, W. Dong, T. Wang, G. Meng and X. Zhu, *J. Alloys Compd.*, **484**, 619 (2009); https://doi.org/10.1016/j.jallcom.2009.05.001
12. N. Dupont, A. Kaddouri and P. Gelin, *J. Sol-Gel Sci. Technol.*, **58**, 302 (2011); https://doi.org/10.1007/s10971-010-2391-6
13. D. Li, X. Fang, W. Dong, Z. Deng, R. Tao, S. Zhou, J. Wang, T. Wang, Y. Zhao and X. Zhu, *J. Phys. D Appl. Phys.*, **42**, 055009 (2009); https://doi.org/10.1088/0022-3727/42/5/055009
14. S. Zhou, X. Fang, Z. Deng, D. Li, W. Dong, R. Tao, G. Meng, T. Wang and X. Zhu, *J. Cryst. Growth*, **310**, 5375 (2008); https://doi.org/10.1016/j.jcrysgro.2008.09.193
15. T.W. Chiu, B.S. Yu, Y.R. Wang, K.T. Chen and Y.T. Lin, *J. Alloys Compd.*, **509**, 2933 (2011); https://doi.org/10.1016/j.jallcom.2010.11.162
16. F. Jlaiel, M. Amami, N. Boudjada, P. Strobel and A.B. Salah, *J. Alloys Compd.*, **509**, 7784 (2011); https://doi.org/10.1016/j.jallcom.2011.04.153
17. F. Jlaiel, M. Amami, P. Strobel and A.B. Salah, *Cent. Eur. J. Chem.*, **9**, 953 (2011); https://doi.org/10.2478/s11532-011-0073-z
18. M. Amami, V.C. Colin, P. Strobel and A.B. Salah, *Physica B*, **406**, 2182 (2011); https://doi.org/10.1016/j.physb.2011.03.027
19. K.C. Ghosh, R.S. Popuri, U.T. Mahesh and K.K. Chattopadhyay, *J. Sol-Gel Sci. Technol.*, **52**, 75 (2009); https://doi.org/10.1007/s10971-009-1999-x

20. M. Lalanne, A. Barnabe, F. Mathieu and P. Tailhades, *Inorg. Chem.*, **48**, 6065 (2009); https://doi.org/10.1021/ic900437x
21. S. Saadi, A. Bouguelia and M. Trari, *Sol. Energy*, **80**, 272 (2006); https://doi.org/10.1016/j.solener.2005.02.018
22. S. Bassaid, M. Chaib, S. Omeiri, A. Bouguelia and M. Trari, *J. Photochem. Photobiol. Chem.*, **201**, 62 (2009); https://doi.org/10.1016/j.jphotochem.2008.09.015
23. M. Amami, S. Smari, K. Tayeb, P. Strobel and A.B. Salah, *Mater. Chem. Phys.*, **128**, 298 (2011); https://doi.org/10.1016/j.matchemphys.2011.03.021
24. H. Huang, K. Liu, K. Chen, Y. Zhang, Y. Zhang and S. Wang, *J. Phys. Chem. C*, **118**, 14379 (2014); https://doi.org/10.1021/jp503025b
25. N.A. Banerjee, S. Kundoo and K.K. Chattopadhyay, *Thin Solid Films*, **440**, 5 (2003); https://doi.org/10.1016/S0040-6090(03)00817-4
26. L. Pan, X. Liu, Z. Sun and C.Q. Sun, *J. Mater. Chem. A Mater. Energy Sustain.*, **1**, 8299 (2013); https://doi.org/10.1039/c3ta10981j